

Article

# Research of Energy and Ecological Indicators of a Compression Ignition Engine Fuelled with Diesel, Biodiesel (RME-Based) and Isopropanol Fuel Blends

Alfредas Rimkus <sup>1,2</sup> , Jonas Matijošius <sup>2,3,\*</sup>  and Sai Manoj Rayapureddy <sup>2</sup>

<sup>1</sup> Department of Automobile Transport Engineering, Technical Faculty, Vilnius College of Technologies and Design, Olandų g. 16, LT-01100 Vilnius, Lithuania; a.rimkus@vtdko.lt

<sup>2</sup> Department of Automobile Engineering, Faculty of Transport Engineering, Vilnius Gediminas Technical University, J. Basanavičiaus g. 28, LT-03224 Vilnius, Lithuania; sai-manoj.rayapureddy@stud.vgtu.lt

<sup>3</sup> Institute of Mechanical Science, Vilnius Gediminas Technical University, Basanavičiaus g. 28, LT-03224 Vilnius, Lithuania

\* Correspondence: jonas.matijosius@vgtu.lt; Tel.: +370-684-041-69

Received: 27 March 2020; Accepted: 6 May 2020; Published: 11 May 2020



**Abstract:** This article presents the results of a study of energy and ecological indicators at different engine loads (*BMEP*) adjusting the Start of Injection (*SOI*) of a Compression Ignition Engine fuelled with blends of diesel (D), rapeseed methyl ester (RME)-based biodiesel and isopropanol (P). Fuel blends mixed at D50RME45P5, D50RME40P10 and D50RME30P20 proportions were used. Alcohol-based fuels, such as isopropanol, were chosen because they can be made from different biomass-based feedstocks and used as additives with diesel fuel in diesel engines. Diesel fuel and its blend with 10% alcohol have almost the same thermal efficiency (*BTE*). In further examination of energy and ecological indicators, combustion parameters were analysed at *SOI* 6 CAD BTDC using *AVL BOOST* software (*BURN* subprogram). Increasing alcohol content in fuel blends led to a reduced cetane number, which prolonged the ignition delay phase and intensified heat release in the premixed combustion phase. Higher combustion temperatures and oxygen content in the fuel blends increased  $\text{NO}_x$  emissions. Lower C/H ratios and higher  $\text{O}_2$  levels affected by RME and isopropanol reduced smoke emissions.

**Keywords:** compression ignition (CI) engine; biodiesel; isopropanol; combustion; energy indicators; ecological indicators

## 1. Introduction

The rising demand for fossil fuels and the environmental issues concerning their use are the biggest challenges that people face today. The transportation sector alone contributes up to 30% of the world's harmful emissions [1]. As the demand for fossil fuels continues to rise faster than its supply, fossil fuels deplete, which in turn drives the price of such fuels as diesel and petrol up [2–4]. The absence of a replacement for vehicles that run on liquid fuels, and a high price of electric vehicles made the automotive industry devote its resources to finding alternative fuels as a replacement and to decreasing the emissions concerned with environmental problems [5–7]. Recent studies revealed that greenhouse gases and harmful combustion chamber emissions can be significantly reduced by using fuels, such as alcohol and biodiesel, as primary alternatives [8–16].

In order to beat the fossil fuel deficiency and control the increasing demand of natural gas, opportunities for using alternative fuels in internal combustion engines have been searched [17]. The ease of handling and storing alcohol and biodiesel makes them promising substitutes for fossil fuels [9,18–21].

Modern biofuel production technologies are sufficiently developed and focused on the production of alcohols, which are very widely used as fuel additives [22]. Mostly ethanol is produced, the production technologies of which have been well known since ancient times. As a fuel additive ethanol has many disadvantages, the most important of which is its corrosivity [23]. Therefore, the selection of an alternative fuel blend for these studies focused on propanol, which is less corrosive and is close to petroleum diesel in its properties and calorific value [24]. In addition, when blended with diesel (10% v/v), propanol performs better in terms of emissions and noise than ethanol [25]. This choice was also based on its cheapness compared to other higher order alcohols like butanol and pentanol [26].

The use of alternative fuels in standard internal combustion engines most often requires modifying such engines. Our proposed three-component fuel mixture allows the replacement of conventional fuels (diesel) with alternative analogues, the use of biodiesel must take into account many operational aspects, such as e.g., *CFPP*, and alcohol propanol allows one to partially solve this problem. Therefore, the chosen three-component diesel-biodiesel-propanol blend allows us to solve the difficult task of using alternative fuels without engine modifications. The three-component mixtures mentioned are rarely found in the literature and are usually defined by a narrow analysis of fuel consumption and some exhaust parameters, and a more detailed analysis of heat release and other parameters is postponed for further research [27].

The performance of the diesel engine with the blend of *n*-propanol at different proportions like 10% by volume is attainable [28]. Diesel engines can use propanol-diesel blends containing 10 to 20% propanol without significantly affecting engine performance. It is further concluded that 10–20% of propanol-diesel blends are beneficial in reducing harmful fumes and  $\text{NO}_x$  emissions [29]. *n*-Propanol/diesel blends higher than 30% showed lower soot density due to the predominant effect of increasing spontaneous oxygen content in *n*-propanol/diesel mixtures [30].

It was observed that when the isopropanol concentration exceeds 15%, the combustion temperature and *BTE* performance starts to increase in biodiesel [31], especially in biodiesel-diesel-isopropanol blends (80%/10%/10%) [27]. Isopropanol improves the cold-flow limit in blends with both diesel and biodiesel, cooling it when operating at low temperatures [32]. 15% Isopropanol content in diesel allows for improved engine performance, lower smoke and  $\text{NO}_x$  emissions (at low to medium loads), but increases brake specific fuel consumption (*BSFC*) due to its lower calorific value [33]. Increasing the isopropanol content to 55% compared to diesel led to an increase in nitrogen oxide emissions (by an average of 139%), a reduction in carbon monoxide emissions (45%) and an increase in  $\text{CO}_2$  emissions (by an average of 17%). However, no significant change in unburnt hydrocarbon emissions was observed [34].

Mixing different alcohols (ethanol-isopropanol and butanol) (*EPB*) with diesel at the ratio of 20 and 40% did not demonstrate a significant increase in heat release and combustion pressure compared to that of diesel. They have been found to have a lower molecular weight flux permeability than diesel, and the flame light index was lower with the use of the aforementioned additives in diesel, which contributed to lower soot emissions [35]. On the other hand, this led to a shorter initial combustion duration (*ICD*) and major combustion duration (*MCD*) conditions [11]. Changing injection strategies for *EPB* blends revealed that pilot injection reduces the heat release rate and the peak pressure, while dual injection improves fuel economy, reduces  $\text{NO}_x$  emissions, at the same time increasing soot [35].

The blend of 30% *EPB* alcohols with gasoline improves *BTE* and slightly increases  $\text{CO}$  (4.2%), hydrocarbon ( $\text{HC}$ ) (18.9%) and  $\text{NO}_x$  emissions (5.5%) compared to mineral gasoline [36]. Correspondingly, adding 1% of water to *EPB* blends (10% *EPB* and 90% mineral gasoline) resulted in an even better ecological effect—a decrease in  $\text{CO}$  of up to 7.5% and in  $\text{NO}_x$  of up to 12.4%, respectively [12]. The emulsion blend of fuel and water reduces local areas where the maximum temperature is reached, resulting in decreased nitrogen activity and  $\text{NO}_x$  concentration [37]. However, using isopropanol additive in gasoline alone significantly increases  $\text{HC}$  emissions at low inlet air temperatures with increasing isopropanol concentration in isopropanol-gasoline blends [38].

When using 25% isopropanol in petrol blends with combustion control, there is a direct relationship between octane number and combustion parameters of isopropanol. Start of combustion (SOC) is delayed by increasing isopropanol content in the blend because isopropanol is more resistant to jerky engine operation [39]. By reducing spark time in a petrol engine, isopropanol-gasoline blends (with isopropanol content up to 30%) had lower NO<sub>x</sub> emissions than those found at the initial spark time [40].

Oxygen content is the key parameter that differs in fossil fuels and biodiesel [41–43]. Environmentally friendly biodiesel produces clean and renewable energy, thus making it the alternative hope [44–46]. A study found that rapeseed methyl ester (RME) produced lower CO<sub>2</sub> emissions due to a lower carbon-to-hydrogen ratio as compared to diesel [47]. Methanol, ethanol are most commonly used in fuel blends with biodiesel, and currently the second ACB wave will make butanol cheaper [48]. The use of propanol in fuel blends with biodiesel is a rare case, determined by the greater development of other alcohol production technologies [20,49]. Lower heating values for B90Pr10 (90% biodiesel and 10% propanol fuel mixtures) and cetane number increased BSFC and fuel gas temperatures while reducing BTE [50]. Table 1 lists the properties of pure diesel, RME and isopropanol [51].

**Table 1.** Properties of 100% pure diesel, rapeseed methyl ester and isopropanol.

Properties	Diesel	Rapeseed Methyl Ester	Isopropanol
Density ( $kg/m^3$ )	843	877	785.1
Mass Fraction (% mass): Carbon	86.3	77.5	60
Hydrogen	13.7	12	13.4
Oxygen	0	10.5	26.6
Stoichiometric AFR	14.3	12.5	10.4
Lower Heating Value (LHV)(MJ/kg)	42.3	37.8	32.8
Cetane number	51	48	12
Auto-ignition temperature (°C)	250	240	399

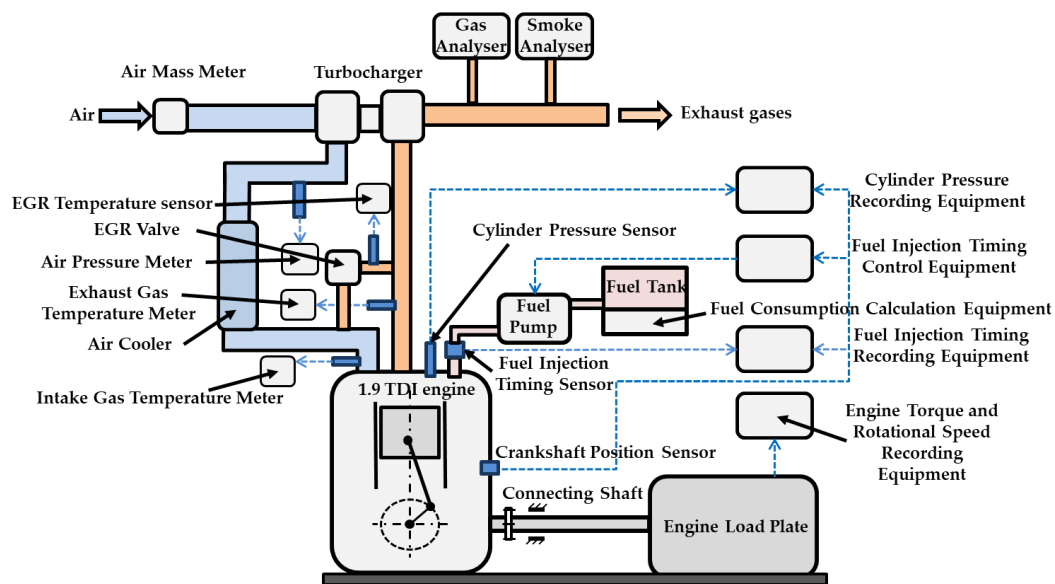
The aim of the research is to reveal the performance, combustion and emission characteristics of IC engines using pure diesel and fuel blends with different proportions of diesel, rapeseed methyl ester-based biodiesel and isopropanol.

## 2. Materials and Methods

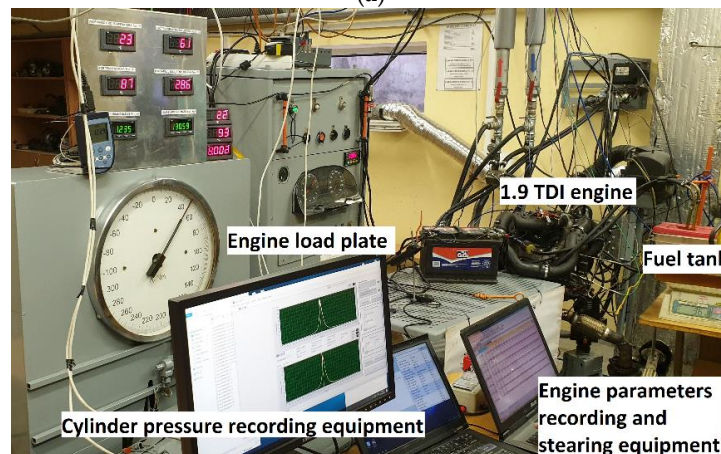
### 2.1. Engine Testing Equipment

The engine used for testing is a 1.9 Turbocharged Direct Injection (TDI) diesel engine with a VP37 (BOSCH, Stuttgart, Germany) electronic controlled distribution type fuel pump. The start of the injection (SOI) was controlled by the Engine Electronic Control Unit (ECU) and it was a single injection strategy. Figure 1 presents a detailed image of the tested engine and its parts, while research conducted by other authors [52–55] and Table 2 lists the test engine parameters.

The brake torque  $M_B$  (Nm) was determined on a load bench with a measurement error of  $\pm 1.2$  Nm. Hourly fuel consumption  $B_f$  (kg/h) was found using electronic scales SK-5000 with a 0.5% measurement error. The pressure in the cylinder was measured using a piezoelectric sensor GG2-1569 mounted on a glow plug with a sensitivity of  $15.8 \pm 0.09$  pC/bar. Cylinder pressure values were recorded using the LabView Real software at an interval of 0.176 CAD. The pressure in the engine intake manifold was measured using an OHM HD 2304.0 pressure gauge (Delta, Padova, Italy) with a measurement error of  $\pm 0.0002$  MPa. The intake air and the exhaust gas temperature were measured using K-type thermocouples IR 8839 accurate to  $\pm 1.5$  °C. The exhaust gas concentration was determined using a DiCom 4000 gas analyzer (AVL, Graz, Austria). CO<sub>2</sub> measurement accuracy was 0.1% vol., CO—0.01% vol., HC—1 ppm, NO<sub>x</sub>—1 ppm, and smoke absorption coefficient—0.01 m<sup>-1</sup>.



(a)



(b)

Figure 1. Image of the test engine: (a) test bench scheme; (b) test rig.

Table 2. Main parameters of the 1.9 TDI diesel engine.

Parameter	Value
Displacement ( $cm^3$ )	1896
No. of cylinders	4
Compression ratio	19.5
Power ( $kW$ )	66 (4000 rpm)
Torque ( $Nm$ )	180 (2000–25,000 rpm)
Bore ( $mm$ )	79.5
Stroke ( $mm$ )	95.5
Intake valve opening at	13 CAD before TDC
Intake valve closing at	25 CAD after BDC
Exhaust valve opening at	28 CAD before BDC
Exhaust valve closing at	19 CAD after TDC
Fuel injection	Direct injection (single)
Fuel injection-pump design	Axial-piston distributor injection pump
Nozzle type	Hole-type
Nozzle and holder assembly	Two-spring
Nozzle opening pressure ( $bar$ )	200

Statistical calculations of type A uncertainties were used to measure exhaust. Type A uncertainties were used to determine the standard deviation for repeated measurements, where  $u(x)$  is uncertainty,  $n$ —repeatability of measurements, and  $s(\bar{x})$ —reliability [55,56]:

$$u(x) = s(\bar{x}) = \frac{s(x)}{\sqrt{n}} \quad (1)$$

where  $\bar{x}$  is the mean repeated value;  $s(x)$  is a standard deviation;  $s(\bar{x})$  is a standard deviation of the mean. Uncertainty ranges  $u(x)$  of exhaust components are presented in Table 3.

**Table 3.** Uncertainty ranges  $u(x)$  of exhaust components.

Exhaust Component	Number of Cycles	$\bar{x}$	Standard Uncertainty $u(x)$
CO (g/kWh)	4	830	0.0036
CO <sub>2</sub> (g/kWh)	4	895	0.0041
HC (g/kWh)	4	0.07	0.0005
NO <sub>x</sub> (g/kWh)	4	13.5	0.0079
Smoke (m <sup>-1</sup> )	4	7.3	0.0026

## 2.2. Fuels and Test Conditions

Tests were conducted using 100% pure diesel fuel and fuel blends prepared using different proportions of diesel (D), rapeseed methyl ester (RME)-based biodiesel and isopropanol (P). The first blend contained 50% diesel, 30% rapeseed methyl ester and 20% isopropanol (D50RME30P20), the second blend had 50% diesel, 40% rapeseed methyl ester and 10% isopropanol (D50RME40P10), and the third one 50% diesel, 45% rapeseed methyl ester and 5% isopropanol (D50RME45P5). The properties like density, mass fraction and lower heating value of the blends were calculated using the following formula:

$$\text{properties of fuel blends} = \sum [(\text{percentage of fuel blend} \times \text{property})] \quad (2)$$

Table 3 presents a comparison of the calculated properties of the fuel blends with the standard diesel fuel. Uncertainties were calculated according to the model B [55]. Standard uncertainties were calculated according to the formula:

$$u_c = \sqrt{u_c^2(f)} \quad (3)$$

where  $u_c^2(f)$  is the total uncertainty dispersion.

The uncertainty calculations for each fuel blend are presented in Table 4.

**Table 4.** Comparison of fuel properties of different fuel blends used and uncertainty ranges  $u_c$  of each fuel blend parameter.

	D100	D50RME45P5	D50RME40P10	D50RME30P20
Density (kg/m <sup>3</sup> )	843	855.4	850.8	844.4
$u_c$ of Density (kg/m <sup>3</sup> )	0.008	0.0037	0.0032	0.0026
Mass Fraction (%): Carbon	86.3	81.025	80.15	78.4
$u_c$ of Carbon (%)	0.00333	0.00322	0.00215	0.00203
Hydrogen	13.7	12.92	12.99	13.13
$u_c$ of Hydrogen	0.00064	0.00058	0.00047	0.00044
Oxygen	0	6.055	6.86	8.47
$u_c$ of Oxygen	0	0.00008	0.00009	0.00012
Lower Heating Value (MJ/kg)	42.3	39.8	39.55	39.05
$u_c$ of Lower Heating Value (MJ/kg)	0.00814	0.00726	0.00633	0.00589
Cetane Number (-)	51	34.49	31.84	27.94
$u_c$ of Cetane Number (-)	0.0255	0.0344	0.0467	0.0592

Engine tests were carried out at the engine speed of  $n = 2000$  rpm and engine brake torque  $M_B$  was 30, 60 and 90 Nm, which corresponds to the Brake Mean Effective Pressure (*BMEP*) 0.2 MPa, 0.4 MPa and 0.6 MPa in the first experimental tests step. These are the loads of a city car running of the  $\approx 50$  km/h,  $\approx 80$  km/h and  $\approx 100$  km/h speeds. During load-changing tests, fuel Start or Injection Timing (*SOI*  $\approx 2$  CAD BTDC) was controlled by the engine electronic control unit. There were (*BMEP* = 0.3 MPa) injection timing was adjusted (*SOI* = 0 . . . 16 CAD BTDC) by modulating the *SOI* control signal in the second experimental test step. Injection timing was adjusted to determine the variation of engine performance using fuel mixtures of different properties under different combustion conditions. The Energy Indicators (Hourly Fuel Consumption  $B_f$ , Brake Specific Fuel Consumption *BSFC*, Brake Thermal Efficiency (*BTE*)) and Ecological Indicators (emission of carbon monoxide CO, carbon dioxide CO<sub>2</sub>, nitrogen oxides NO<sub>x</sub>, hydrocarbons CH, and smoke) were measured and calculated at different engine loads and by adjusting start of injection. The results of all the tested fuel blends will be analysed comparing them with results of diesel fuel. Experimental tests were performed to ensure repeatability of the experiments. Several experiment design parameters were singled out, such as fuel type used, engine rotation speed, engine load torque, and fuel injection angle.

The density difference between the fuels was found to decrease with increasing alcohol concentration as seen in Table 4. Since the molecular mass of alcohols is lower than that of diesel and biodiesel [57–60], with the alcohol content increasing from 5% to 10%, the density was found to decrease by 1.45%, and with an additional increase from 10% to 20%, the density decreased by nearly 0.17%. When compared to diesel, fuel blends with a 5 and 10% alcohol content tended to be denser, and the D50RME30P20 blend tended to have a lower density compared to conventional fuel as calculated and presented in Table 4.

A lower heat value was found to differ less with an increase in the alcohol percentage share as seen in Table 4. The lower heat value difference increased to 6.5% when increasing the fuel concentration from 5% to 10%, and a further change of the concentration from 10% to 20% led to the difference increasing by nearly 7.7%. The lower heat value highly depends on carbon and hydrogen content in fuel [61–63]. So, with a relatively higher carbon and hydrogen content in diesel compared to their content in other fuel blends, the lower heat value of conventional fuel was found to be higher than that of other fuel blends, which declined with increasing alcohol content as seen in Table 4.

The difference in the cetane number decreased with increasing alcohol content as seen in Table 4. The conventional diesel fuel is known for being rich in paraffin, which helps it achieve a higher cetane number compared to other fuel blends [64]. When increasing the alcohol content from 5% to 10%, the difference was found to increase to 37.5%, and a further increase in alcohol content to 20% led to an increase in the difference of nearly 45%. As seen in Table 4, the cetane number steadily decreased with alcohol content compared to that of the conventional fuel. The fuel stability was ensured by producing fuel blends right before testing and feeding them to the engine.

### 2.3. Tools for Numerical Analysis of the Combustion Process

Due to a significant change in the cetane number in diesel and other prepared fuel blends, analysing changes in performance of the engine by calculating combustion characteristics and comparing them with those of diesel is necessary. *AVL BOOST* software was used in calculating the combustion characteristics with the help of *BURN* subprogram. *BURN* analysis was conducted having created a digital model of the 1.9 TDI diesel engine used in the experiment as seen in Figure 2. The digital model of the engine was constructed by selecting the required elements from a displayed element catalogue in *AVL BOOST*. The analysis of combustion requires general data on engine parameters, fuel and data describing the operating point.

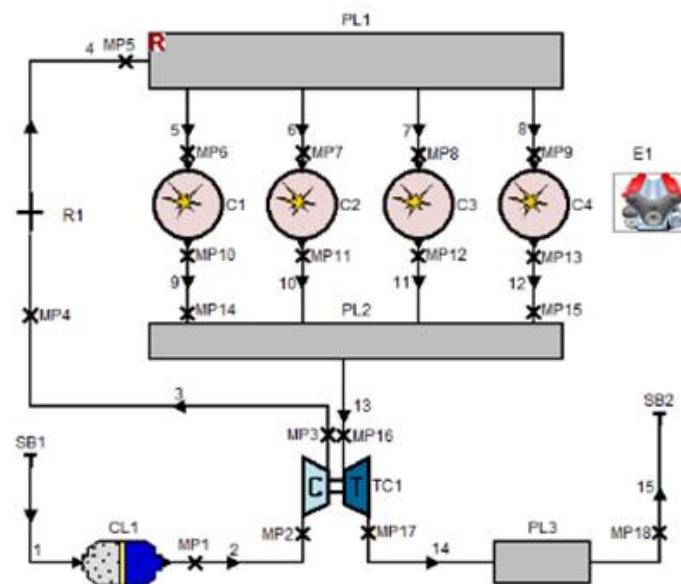


Figure 2. Digital Engine Model used in AVL BOOST.

Engine parameters and experiment results were uploaded in the BURN subprogram and run to get the combustion characteristics. Changes in the in-cylinder pressure and temperature, heat release rate (ROHR) and the mass fraction burnt (MFB) were calculated in this research:

$$ROHR = \frac{dx}{d\alpha} = \frac{6.908}{\alpha_{CD}} \cdot (m_v + 1) \cdot \left( \frac{\alpha - \alpha_{SOC}}{\alpha_{CD}} \right)^{m_v} \cdot e^{-6.908 \cdot \left( \frac{\alpha - \alpha_{SOC}}{\alpha_{CD}} \right)^{(m_v+1)}} \quad (4)$$

$$dx = \frac{dQ}{Q} \quad (5)$$

$$MFB = \int_{\alpha_{SOC}}^{\alpha} \frac{dQ}{d\alpha \cdot Q(\alpha)} \cdot d\alpha = 1 - e^{-6.908 \cdot \left( \frac{\alpha - \alpha_{SOC}}{\alpha_{CD}} \right)^{(m_v+1)}}, \quad \alpha > \alpha_{SOC} \quad (6)$$

where  $Q$ —total fuel heat input;  $\alpha$ —crank angle;  $m_v$ —combustion shape parameter;  $\alpha_{SOC}$ —start of combustion;  $\alpha_{CD}$ —combustion duration.

### 3. Results and Discussion

The experimental tests were carried out in two steps: (a) changing the engine load  $BMEP$  (0.2; 0.4 and 0.6 MPa); (b) changing  $SOI$  (0 ... 16 CAD BTDC), and  $BMEP = 0.3$  MPa. After plotting the graphs from the (b) experiment results, a polynomial curve was drawn with a degree of 2 for all the energy and ecological parameters to get a change trend.

#### 3.1. Energy Indicators

Brake Specific Fuel consumption (BSFC) of diesel fuel was low at all loads compared to other fuel blends, as observed in Figure 3a. When increasing alcohol content, fuel consumption tended to increase with D50RME30P20 being at the maximum. Having replaced 50% of diesel by a blend of biodiesel and propanol and increased the concentration of propanol up to 20% (D50RME30P20), BSFC increased ~9% due to a 7.7% reduction in LHV (Table 4) and a change in combustion process. With  $BMEP = 0.3$  MPa, the analysis of BSFC from the perspective of injection timing revealed a higher consumption of all the fuel blends (7–10%), and with advancing angle, the value tended to decrease and further increase after 8–12 CAD BTDC as seen in Figure 3b.

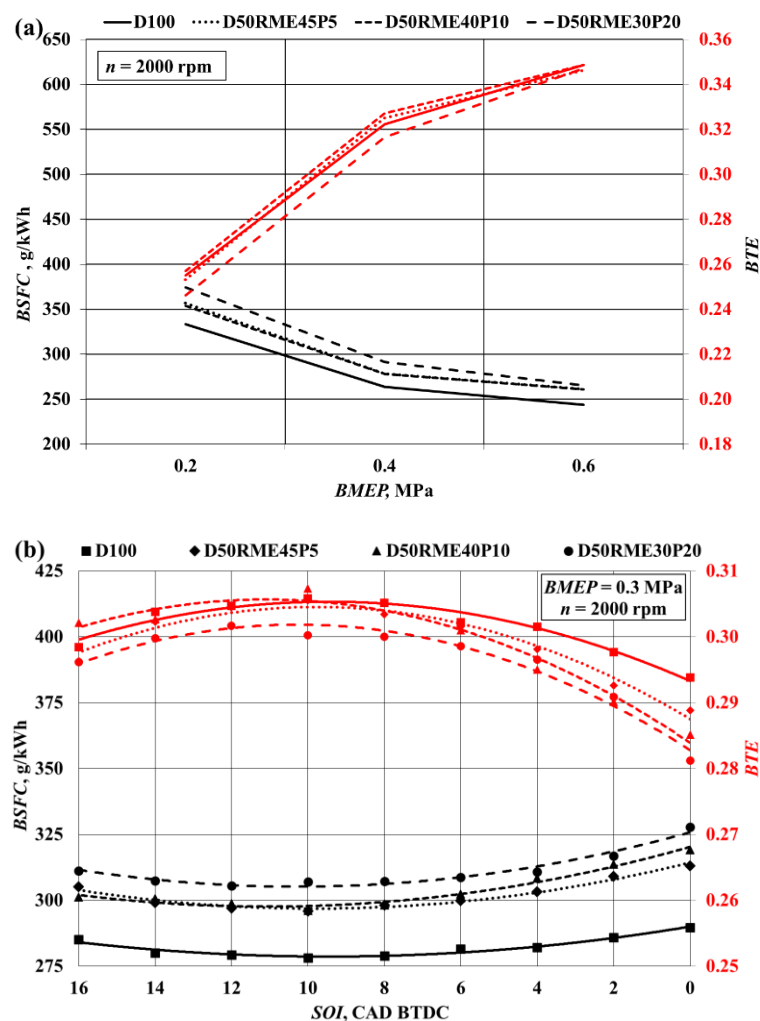


**Figure 3.** Dependence of Brake Specific Fuel Consumption and Brake Thermal Efficiency on different: (a) loads; (b) injection timing.

At 8 CAD BTDC, D100 fuel was at its lowest on average. The lowest consumption of D-RME-P blends was achieved with injection timing of 10...12 CAD BTDC, as the cetane number of this fuel decreased to 23.06.

*BTE* of D50RME45P5 and D50RME40P10 fuel blends at *BMEP* 0.2 and 0.4 MPa was close to that of diesel, and *BTE* of D50RME30P20 was 3.5% (at *BMEP* 0.2 MPa) to 1.8% (at *BMEP* 0.4 MPa) lower as seen in Figure 3a. With a *BMEP* = 0.6 MPa, *BTE* of all fuels was slightly different and reached up to 0.35%.

Observing the dependence curve of efficiency on injection timing in Figure 3b, at *BMEP* = 0.3 MPa, *BTE* of the D50RME30P20 fuel blend was ~1.8% lower than that of diesel. *BTE* of fuel blends with 5% and 10% isopropanol content was lower (2.5 ... 1.2%) at *SOI* = 0 ... 6 CAD BTDC, but at *SOI* = 8 ... 12 CAD BTDC, *BTE* of D50RME45P5 and D50RME40P10 was the same as *BTE* of D100.

### 3.2. Ecological Indicators

Carbon dioxide comparative emissions (g/kWh) were found to decrease for all the fuels with increasing load as seen in Figure 4a as *BTE* increased and *BSFC* decreased. At a low load (*BMEP* = 0.2 MPa),  $\text{CO}_2$  emissions of the blends containing isopropanol were 0.8 ... 1.9% higher compared to diesel but increasing the load to *BMEP* = 0.6 MPa resulted in ~0.8% lower  $\text{CO}_2$  emissions for the D50RME40P10 fuel blend.

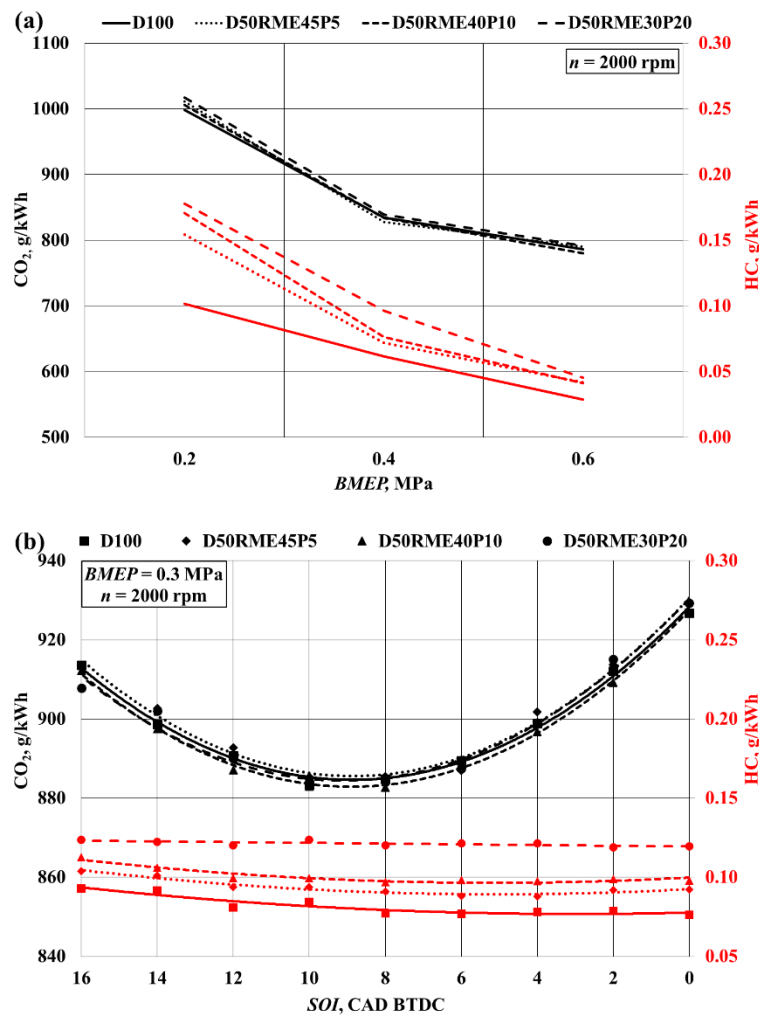


**Figure 4.** Dependence of carbon dioxide emissions and hydrocarbons on different: (a) loads; (b) injection timing.

This was due to a 2.1% decrease in the C/H ratio (Table 4) and the fact that at higher loads the *BTE* of all fuels was similar. Checking the dependence of emissions on injection timing revealed that all the fuels showed a gradual decrease in emissions with advancing injection timing as seen in Figure 4b, *BTE* increased, and smoke emissions decreased (Figure 5b). Diesel was found to have similar CO<sub>2</sub> emissions compared to emissions of other fuel blends. CO<sub>2</sub> emissions of the D50RME40P10 fuel blend at various *SOIs* were only ~0.2% lower than emissions of D100. Even though RME and C/H ratio of isopropanol is lower, increased fuel consumption increases CO<sub>2</sub> emissions.

Hydrocarbon emissions of all the fuels were found to decrease with increasing load as seen in Figure 4a, as the combustion temperature increased [65,66]. Having the lowest emissions as compared to all the other fuels, diesel also tended to have a steady decrease pattern of ~38%, ~45% and ~60% (compared to the D50RME45P5, D50RME40P10 and D50RME30P20 fuel blends in hydrocarbon emissions). When increasing the alcohol content, fuel blends tended to have higher hydrocarbon emissions due to increasing alcohol base of the fuel, however, HC emissions were low compared to petrol engine [52]. The observation of the dependence of hydrocarbon emissions on injection timing revealed that with an increase in alcohol content, emissions tended to increase as seen in Figure 4b. HC emissions of D50RME45P5, D50RME40P10 and D50RME30P20 increased by ~15%, ~28% and ~58% compared to D100 at *SOI* ≈ 6 CAD BTDC. With the engine running on all the fuels, hydrocarbon emissions showed a slight growth trend when injection timing was advanced more than 6 CAD BTDC.

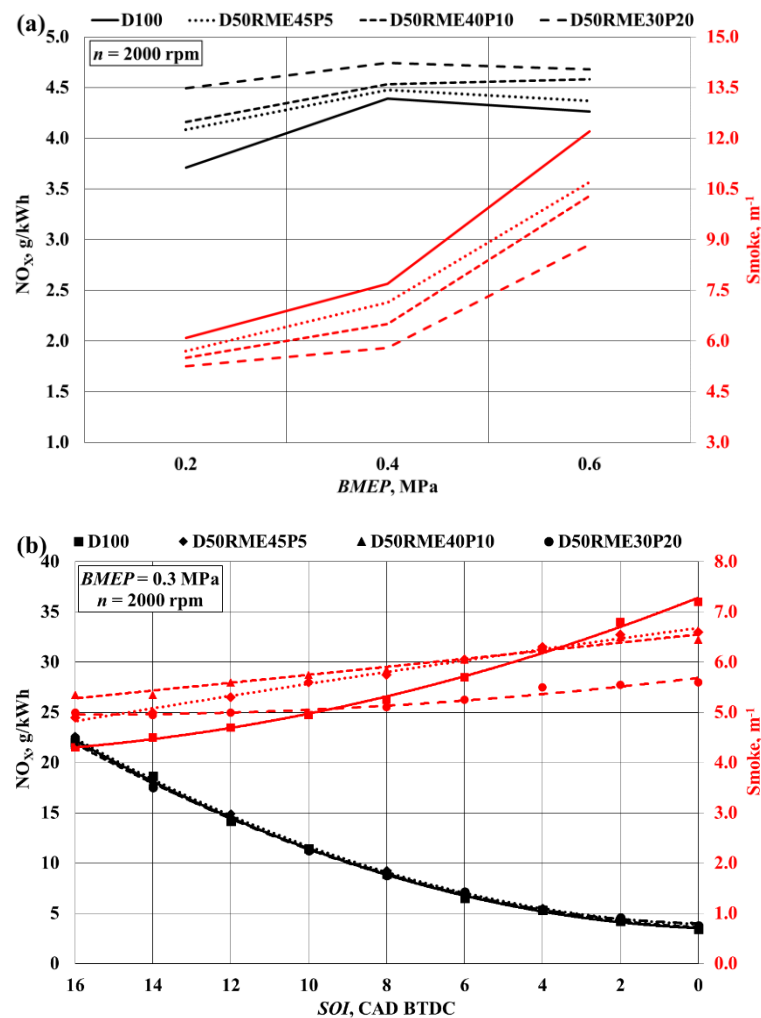


Figure 5. Dependence of nitrogen oxide emissions and smoke on different: (a) loads; (b) injection timing.

Nitrogen oxide emissions for D50RME45P5, D50RME40P10, D50RME30P20 at a low load ( $BMEP = 0.2$  MPa) were  $\sim 10\%$ ,  $\sim 12\%$ , and  $\sim 21\%$  higher compared to those of D100 fuel as seen in Figure 5a. This was mainly due to the increased ignition delay due to a low cetane number of isopropanol (see the Dependence of the rate of heat release and the mass burnt fraction on the crank angle degree figure below.) and the increased oxygen concentration in the fuel blend (Table 4).

With an increase in the load ( $BMEP = 0.6$  MPa), the difference in  $\text{NO}_x$  emissions was reduced to  $\sim 4\%$ ,  $\sim 7\%$  and  $\sim 10\%$  as the effect of ignition delay on different fuels was reduced. While analysing the dependence of nitrogen oxide emissions on the injection timing, emissions were found to rise steadily with increasing injection timing as seen in Figure 5b, because combustion occurred at a lower volume and higher temperatures [67]. All the fuels were found to follow a similar pattern, but after a more careful analysis, diesel emissions were found to be lower (1 ... 4%) compared to emissions of other fuel blends. An earlier injection timing reduced the difference between  $\text{NO}_x$  emissions of diesel and fuel blends [68–70].

The smoke level of fuels tended to increase with increasing load as seen in Figure 5a, as fuel mass increases per cycle and the air-to-fuel ratio decreases. Increasing the isopropanol concentration in fuel blends reduces smoke level, and this effect is more intense with an increasing engine load [71]. At a low load ( $BMEP = 0.2$  MPa), the D50RME45P5, D50RME40P10 and D50RME30P20 fuel smoke emissions decreased by  $\sim 6\%$ ,  $\sim 10\%$  and  $\sim 14\%$ , respectively, in comparison to pure diesel. Higher oxygen concentrations and lower C/H ratios resulted in lower D50RME30P20 smoke emissions. Increasing the load to  $BMEP = 0.6$  MPa increased the smoke reduction effect to  $\sim 12\%$ ,  $\sim 16\%$ .

The analysis of the dependence of smoke levels on injection timing revealed that the levels tended to decrease with advancing the injection timing as seen in Figure 5b. Interestingly, throughout the SOI study range (0...16 CAD BTDC), the combustion performance resulted in the largest reduction in diesel smoke emissions from  $\sim 7.25 \text{ m}^{-1}$  to  $\sim 4.25 \text{ m}^{-1}$  ( $\sim 40\%$ ), while the D50RME30P20 smoke emissions decreased from  $\sim 5.7$  to  $\sim 5 \text{ m}^{-1}$  ( $\sim 12\%$ ). Therefore, at  $\text{SOI} = 0\text{...}8 \text{ CAD BTDC}$  (low advanced injection timing), D50RME30P20 had the lowest smoke emissions, and at  $\text{SOI} = 10\text{...}16 \text{ CAD BTDC}$  (high advanced injection timing), smoke emissions of D100 fuel were the lowest.

### 3.3. Combustion Characteristics

The analysis of combustion characteristics was conducted with the engine operating at  $\text{BMEP} = 0.3 \text{ MPa}$  ( $n = 2000 \text{ rpm}$ ). Changing SOI (0 ... 16 CAD BTDC) allowed comparing energy and ecological performance of the engine running on different fuels (Figures 3b, 4b and 5b) and concluding that with ignition timing being 6 CAD BTDC engine efficiency is close to the maximum, and smoke and  $\text{NO}_x$  emissions are relatively low. The pressure values of all the fuels at  $\text{SOI} = 6 \text{ CAD BTDC}$  obtained during the experiment as seen in Figure 6 were uploaded in the AVL BOOST (BURN subprogram) to get the combustion characteristics. Since the result at  $\text{SOI} = 6 \text{ CAD BTDC}$  was relatively good, the combustion characteristics of fuel blends, such as in-cylinder pressure, pressure rise, rate of heat release (ROHR) and mass fraction burned (MFB), were analysed and compared to those of pure diesel at that particular degree of ignition timing.

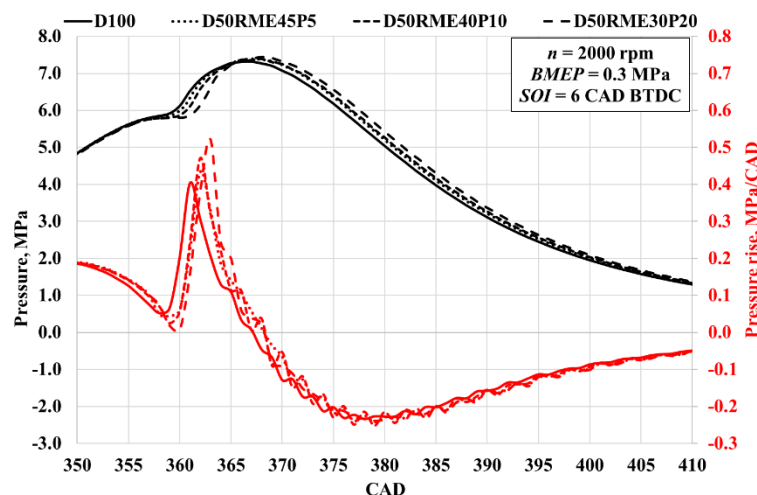


**Figure 6.** Dependence of pressure and pressure rise in the cylinder on the crank angle degree.

Conventional diesel fuel (D100) showed the maximum pressure of  $\sim 7.32 \text{ MPa}$  at 367 CAD, while the maximum pressures of D50RME45P5, D50RME40P10 and D50RME30P20 were  $\sim 1.0\%$ ,  $\sim 1.1\%$  and  $\sim 1.7\%$  higher as seen in Figure 6. There was also a delayed burning with isopropanol.

A combustion-driven pressure starts to increase the earliest with the engine running on diesel. The maximum pressure rise of  $\sim 0.40 \text{ MPa/CAD}$  was observed at 361 CAD as seen in Figure 6. The maximum pressure rise increases with an increase in alcohol percentage.  $\sim 7.5\%$  (361.5 CAD),  $\sim 17\%$  (362 CAD) and  $\sim 29\%$  (363 CAD) was the maximum increase for D50RME45P5, D50RME40P10 and D50RME30P20.

The maximum rate of heat release of diesel fuel was lower at  $32.0 \text{ J/deg}$  than that of other fuel blends as seen in Figure 7. The maximum rate of  $34.8 \text{ J/deg}$  ( $\sim 8\%$  higher) was observed with the D50RME45P5 fuel blend, while the maximum rate of D50RME40P10 was  $38.1 \text{ J/deg}$  ( $\sim 19\%$  higher) and that of D50RME30P20— $46.4 \text{ J/deg}$  ( $\sim 44\%$  higher). Isopropanol reduces the cetane number (Table 4), prolongs the ignition delay phase and significantly increases the maximum ROHR during the premixed combustion phase [58]. The LHV of isopropanol is lower, but this is offset by the higher fuel content

(Figure 7), and the diffusion combustion phase produces a similar amount of heat for all fuels. Higher maximum temperatures during premixed combustion phase increase the formation of nitrogen oxides, but allows for a better combustion of soot at the end of the combustion process [69–71].

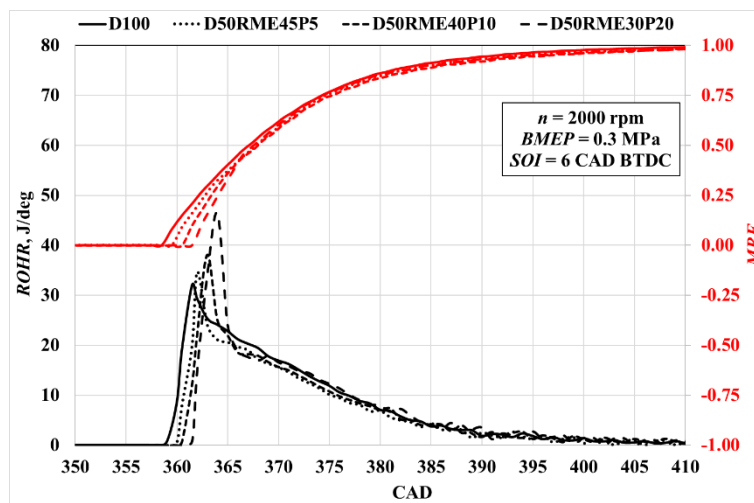


**Figure 7.** Dependence of the rate of heat release and the mass burnt fraction on the crank angle degree.

The mass burn fraction diagram in Figure 7 confirms the prolongation of the ignition delay phase in fuel blends with a higher alcohol content. Ignition delay for D100 was ~5 CAD, D50RME45P5—~6 CAD, D50RME40P10—~7 CAD and D50RME30P20—~8 CAD.

Although ignition delay is longer for blends with isopropanol [72], oxygen concentration in blends significantly increases due to RME and isopropanol. This significantly accelerates the combustion process during the premixed combustion phase, and 0.5 MBF of all fuels is available at ~7.5 CAD ATDC. The diffusion combustion phase MBF intensity is similar for all fuels, although the fuel consumption of D50RME30P20 increased by ~9% (Figure 3), which was offset by increased injection rate due to a lower isopropanol viscosity and faster combustion driven by a higher oxygen concentration. 99% of the D100 fuel mass ends up burning ~410 CAD ATDC, D50RME45P5—~412 CAD ATDC, D50RME40P10—~413 CAD ATDC and D50RME30P20—~414 CAD ATDC.

#### 4. Conclusions

The analysis of the energy, ecological and combustion parameters of diesel 100, D50RME45P5, D50RME40P10 and D50RME30P20 in a turbocharged direct injection diesel engine at the speed ( $n$ ) of 2000 rpm and under various loads and injection timings allows making the following conclusions:

- (1) RME and isopropanol reduce  $LHV$  and the cetane number of fuel blends, but increase the oxygen concentration in the blend and lower the C/H ratio.
- (2) D50RME30P20 brake specific fuel consumption increased by ~9% compared to D100 and  $BTE$  decreased by ~1.8% due to a 7.7% reduction in  $LHV$  and a change in the combustion process. The maximum  $BTE$  of the D50RME40P10 fuel blend was equal to D100 efficiency having advanced the injection timing of the fuel blend ~2 CAD. This offset the increase in the ignition delay due to a low propanol cetane number (~12).
- (3) Carbon dioxide emissions of all fuels are similar, but the best carbon dioxide effect was obtained with the D50RME40P10 fuel blend. At medium loads,  $CO_2$  emissions of this blend declined by ~0.2% compared to diesel, though fuel consumption increased by ~6%, as the C/H ratio of the fuel blend was 2.1% lower. A more advanced injection timing ( $SOI = 8 \dots 10$  CAD BTDC) at the minimum fuel consumption allows achieving lower  $CO_2$  emissions.
- (4) Isopropanol has a greater impact on nitrogen oxide emissions at low loads.  $NO_x$  emissions of D50RME45P5, D50RME40P10 and D50RME30P20 increased by ~10%, ~12% and ~21% due to a

higher oxygen concentration in the blends and a higher combustion temperature. With increasing load, an increase in  $\text{NO}_x$  emissions was lower ( $\sim 4\%$ ,  $\sim 7\%$  and  $\sim 10\%$ ) as a low isopropanol cetane number had a lesser effect on the ignition delay phase and the heat release rate during the premixed combustion phase. With an early injection timing,  $\text{NO}_x$  emissions increased, but the impact of alcohol was lower.

- (5) Having replaced diesel with fuel blends at a low load resulted in a  $\sim 6\%$ ,  $\sim 10\%$  and  $\sim 14\%$  reduction in smoke and an average load reduction of  $\sim 12\%$ ,  $\sim 16\%$  and  $\sim 28\%$ . Smoke was reduced by lower C/H ratios and increased oxygen content in the fuels. As the load increased, the *BTE* of the fuel blends increased more intensively, which further reduced smoke emissions. In the case of early injection timing ( $\text{SOI} = 8 \dots 16$  CAD BTDC), smoke emissions of the fuel blends changed (decreased) less intensively due to changed fuel characteristics compared to pure diesel.
- (6) At a low engine load ( $\text{BMEP} = 0.3$  MPa), the average rotation speed ( $n = 2000$  rpm), the fixed injection timing ( $\text{SOI} = 6$  CAD BTDC) and the replacement of diesel by fuel blends with a higher alcohol content (5%, 10% and 20%) resulted in ignition delay changing from  $\sim 5$  CAD to  $\sim 6$  CAD,  $\sim 7$  CAD and  $\sim 8$  CAD. A greater ignition delay (accumulates more fuel) and a higher oxygen content in fuel during the premixed combustion phase increased the heat release intensity by  $\sim 8\%$ ,  $\sim 19\%$  and  $\sim 44\%$ , which in turn increased the pressure rise by  $\sim 8\%$ ,  $\sim 17\%$  and  $\sim 29\%$  in the thermodynamic load of the crank mechanism. During the diffusion combustion phase, the combustion heat release of all the fuels examined was similar.
- (7) The authors plan to continue research of these three-component blends by increasing the share of alternative fuels in the blends and assessing the impact of the EGR system when using these blends.

**Author Contributions:** Author Contributions: Conceptualization, A.R. and S.M.R.; methodology, A.R., S.M.R. and J.M.; software, S.M.R. and A.R.; formal analysis, A.R. and J.M.; validation, A.R. and S.M.R.; writing—original draft preparation, A.R. and J.M.; writing—review and editing, A.R. and J.M.; supervision, A.R., and J.M.; project administration, J.M. All authors have read and agreed to the published version of the manuscript.

**Funding:** This research received no external funding.

**Acknowledgments:** Part of the combustion characteristics reported in this article were obtained using the engine numerical analysis tool AVL BOOST, acquired by signing a Cooperation Agreement between AVL Advanced Simulation Technologies and the faculty of the Transport Engineering of Vilnius Gediminas Technical University.

**Conflicts of Interest:** The authors declare no conflict of interest.

## Abbreviations and Nomenclature

ACB	Acetoneb—utanol producing process
ATDC	After Top Dead Centre (CAD)
AVL	Anstalt für Verbrennungskraftmaschinen List
BDC	Bottom Dead Center
$B_f$	Fuel mass consumption (kg/h)
<i>BMEP</i>	Brake Mean Effective Pressure (MPa)
<i>BSFC</i>	Brake Specific Fuel Consumption (g/kWh)
BTDC	Before Top Dead Center (CAD)
<i>BTE</i>	Brake Thermal Efficiency
CA	Crank Angle (degree)
CFPP	Cold filter plugging point
CO	Carbon monoxide
$\text{CO}_2$	Carbon dioxide
CN	Cetane Number
CV	Calorific Value
D	Diesel fuel

ECU	Electronic Control Unit
EPB	Ethanol-Propanol and butanol fuel blend
HC	Hydrocarbons
IC	Internal combustion
ICD	Initial combustion duration (CAD)
LHV	Lower Heating Value (MJ/kg)
$M_B$	Brake torque (Nm)
MFB	Mass fraction burned
MCD	Major combustion duration (CAD)
$n$	Rotational speed of the crankshaft (rpm)
NO <sub>x</sub>	Nitrogen Oxide
O <sub>2</sub>	Oxygen
P	Isopropanol
ROHR	Rate of heat release (J/deg)
RME	Rapeseed Methyl Ester
SOI	Start of Injection (CAD)
TDC	Top Dead Center
TDI	Turbocharged Direct Injection

## References

1. Enriquez, A.; Benoit, L.; Dalkmann, H.; Brannigan, C. GIZ Sourcebook 5e Transport and Climate Change. *Tech. Rep.* **2014**. [[CrossRef](#)]
2. Abas, N.; Kalair, A.; Khan, N. Review of fossil fuels and future energy technologies. *Futures* **2015**, *69*, 31–49. [[CrossRef](#)]
3. David, M. The role of organized publics in articulating the exnovation of fossil-fuel technologies for intra- and intergenerational energy justice in energy transitions. *Appl. Energy* **2018**, *228*, 339–350. [[CrossRef](#)]
4. Jia, T.; Dai, Y.; Wang, R. Refining energy sources in winemaking industry by using solar energy as alternatives for fossil fuels: A review and perspective. *Renew. Sustain. Energy Rev.* **2018**, *88*, 278–296. [[CrossRef](#)]
5. Tamilselvan, P.; Nallusamy, N.; Rajkumar, S. A comprehensive review on performance, combustion and emission characteristics of biodiesel fuelled diesel engines. *Renew. Sustain. Energy Rev.* **2017**, *79*, 1134–1159. [[CrossRef](#)]
6. Śładkowski, A. (Ed.) *Ecology in Transport: Problems and Solutions*; Lecture Notes in Networks and Systems; Springer International Publishing: Cham, Switzerland, 2020; Volume 124, ISBN 978-3-030-42322-3.
7. Bureika, G.; Steišūnas, S. Complex Evaluation of Electric Rail Transport Implementation in Vilnius City. *Transp. Probl.* **2016**, *11*, 49–60. [[CrossRef](#)]
8. Bhasker, J.P.; Porpatham, E. Effects of compression ratio and hydrogen addition on lean combustion characteristics and emission formation in a Compressed Natural Gas fuelled spark ignition engine. *Fuel* **2017**, *208*, 260–270. [[CrossRef](#)]
9. Chen, H.; He, J.; Zhong, X. Engine combustion and emission fuelled with natural gas: A review. *J. Energy Inst.* **2019**, *92*, 1123–1136. [[CrossRef](#)]
10. Ghadikolaei, M.A.; Cheung, C.S.; Yung, K.-F. Study of combustion, performance and emissions of diesel engine fueled with diesel/biodiesel/alcohol blends having the same oxygen concentration. *Energy* **2018**, *157*, 258–269. [[CrossRef](#)]
11. Li, Y.; Chen, Y.; Wu, G.; Lee, C.-F.F.; Liu, J. Experimental comparison of acetone-n-butanol-ethanol (ABE) and isopropanol-n-butanol-ethanol (IBE) as fuel candidate in spark-ignition engine. *Appl. Therm. Eng.* **2018**, *133*, 179–187. [[CrossRef](#)]
12. Li, Y.; Chen, Y.; Wu, G.; Liu, J. Experimental evaluation of water-containing isopropanol-n-butanol-ethanol and gasoline blend as a fuel candidate in spark-ignition engine. *Appl. Energy* **2018**, *219*, 42–52. [[CrossRef](#)]
13. Li, G.; Liu, Z.; Lee, T.H.; Lee, C.-F.F.; Zhang, C. Effects of dilute gas on combustion and emission characteristics of a common-rail diesel engine fueled with isopropanol-butanol-ethanol and diesel blends. *Energy Convers. Manag.* **2018**, *165*, 373–381. [[CrossRef](#)]
14. Li, M.; Xu, J.; Xie, H.; Wang, Y. Transport biofuels technological paradigm based conversion approaches towards a bio-electric energy framework. *Energy Convers. Manag.* **2018**, *172*, 554–566. [[CrossRef](#)]

15. Moula, M.E.; Nyári, J.; Bartel, A. Public acceptance of biofuels in the transport sector in Finland. *Int. J. Sustain. Built Environ.* **2017**, *6*, 434–441. [[CrossRef](#)]
16. Yan, X.; Gao, P.; Zhao, G.; Shi, L.; Xu, J.-B.; Zhao, T. Transport of highly concentrated fuel in direct methanol fuel cells. *Appl. Therm. Eng.* **2017**, *126*, 290–295. [[CrossRef](#)]
17. Zefreh, M.M.; Török, Á. Theoretical Comparison of the Effects of Different Traffic Conditions on Urban Road Traffic Noise. *J. Adv. Transp.* **2018**, *2018*, 7949574. [[CrossRef](#)]
18. Hoseinpour, M.; Sadrnia, H.; Tabasizadeh, M.; Ghobadian, B. Evaluation of the effect of gasoline fumigation on performance and emission characteristics of a diesel engine fueled with B20 using an experimental investigation and TOPSIS method. *Fuel* **2018**, *223*, 277–285. [[CrossRef](#)]
19. Jamuwa, D.; Sharma, D.; Soni, S. Experimental investigation of performance, exhaust emission and combustion parameters of stationary compression ignition engine using ethanol fumigation in dual fuel mode. *Energy Convers. Manag.* **2016**, *115*, 221–231. [[CrossRef](#)]
20. Yusri, I.; Mamat, R.; Najafi, G.; Razman, A.; Awad, O.; Azmi, W.H.; Ishak, W.; Shaiful, A. Alcohol based automotive fuels from first four alcohol family in compression and spark ignition engine: A review on engine performance and exhaust emissions. *Renew. Sustain. Energy Rev.* **2017**, *77*, 169–181. [[CrossRef](#)]
21. Zaharin, M.; Abdullah, N.; Najafi, G.; Sharudin, H.; Yusaf, T. Effects of physicochemical properties of biodiesel fuel blends with alcohol on diesel engine performance and exhaust emissions: A review. *Renew. Sustain. Energy Rev.* **2017**, *79*, 475–493. [[CrossRef](#)]
22. Szabados, G.; Bereczky, A. Experimental investigation of physicochemical properties of diesel, biodiesel and TBK-biodiesel fuels and combustion and emission analysis in CI internal combustion engine. *Renew. Energy* **2018**, *121*, 568–578. [[CrossRef](#)]
23. Žaglinskis, J.; Lukács, K.; Bereczky, A. Comparison of properties of a compression ignition engine operating on diesel–biodiesel blend with methanol additive. *Fuel* **2016**, *170*, 245–253. [[CrossRef](#)]
24. Matijošius, J.; Sokolovskij, E. Research into the Quality of fuels and their Biocomponents. *Transport* **2009**, *24*, 212–217. [[CrossRef](#)]
25. Pinzi, S.; Redel-Macías, M.; Candia, D.E.L.; Soriano, J.A.; Dorado, M. Influence of ethanol/diesel fuel and propanol/diesel fuel blends over exhaust and noise emissions. *Energy Procedia* **2017**, *142*, 849–854. [[CrossRef](#)]
26. Bereczky, A. The Past, Present and Future of the Training of Internal Combustion Engines at the Department of Energy Engineering of BME. In *Vehicle and Automotive Engineering*; Jármay, K., Bolló, B., Eds.; Springer Science and Business Media LLC: Cham, Switzerland, 2017; Volume 13, pp. 225–234.
27. Bencheikh, K.; Atabani, A.; Shobana, S.; Mohammed, M.; Uğuz, G.; Arpa, O.; Kumar, G.; Ayanoglu, A.; Bokhari, A. Fuels properties, characterizations and engine and emission performance analyses of ternary waste cooking oil biodiesel–diesel–propanol blends. *Sustain. Energy Technol. Assess.* **2019**, *35*, 321–334. [[CrossRef](#)]
28. Yogesh, P.; Dinesh Sakthi, S.; Aravinth, C.; Sathiyakeerthy, K.; Susenther, M. Performance Test on Diesel-Biodiesel–Propanol Blended Fuels in CI Engine. *IJISRT* **2018**, *3*, 1–6.
29. Muthaiyan, P.; Gomathinayagam, S. Combustion Characteristics of a Diesel Engine Using Propanol Diesel Fuel Blends. *J. Inst. Eng. (India) Ser. C* **2016**, *97*, 323–329. [[CrossRef](#)]
30. Thillainayagam, M.; Venkatesan, K.; Dipak, R.; Subramani, S.; Sethuramasamyraja, B.; Babu, R.K. Diesel reformulation using bio-derived propanol to control toxic emissions from a light-duty agricultural diesel engine. *Environ. Sci. Pollut. Res.* **2017**, *24*, 16725–16734. [[CrossRef](#)]
31. Campos-Fernández, J.; Arnal, J.M.; Gomez, J.; LaCalle, N.; Dorado, M.P. Performance tests of a diesel engine fueled with pentanol/diesel fuel blends. *Fuel* **2013**, *107*, 866–872. [[CrossRef](#)]
32. Atmanli, A.; Atmanli, A. Comparative analyses of diesel–waste oil biodiesel and propanol, n-butanol or 1-pentanol blends in a diesel engine. *Fuel* **2016**, *176*, 209–215. [[CrossRef](#)]
33. Şen, M. The effect of the injection pressure on single cylinder diesel engine fueled with propanol–diesel blend. *Fuel* **2019**, *254*, 115617. [[CrossRef](#)]
34. Jamrozik, A.; Tutak, W.; Pyrc, M.; Gruca, M.; Kocisko, M. Study on co-combustion of diesel fuel with oxygenated alcohols in a compression ignition dual-fuel engine. *Fuel* **2018**, *221*, 329–345. [[CrossRef](#)]
35. Lee, T.H.; Hansen, A.C.; Li, G.; Lee, T. Effects of isopropanol-butanol-ethanol and diesel fuel blends on combustion characteristics in a constant volume chamber. *Fuel* **2019**, *254*, 115613. [[CrossRef](#)]

36. Li, G.; Lee, T.H.; Liu, Z.; Lee, C.-F.F.; Zhang, C. Effects of injection strategies on combustion and emission characteristics of a common-rail diesel engine fueled with isopropanol-butanol-ethanol and diesel blends. *Renew. Energy* **2019**, *130*, 677–686. [[CrossRef](#)]
37. Chybowski, L.; Laskowski, R.; Gawdzińska, K. An overview of systems supplying water into the combustion chamber of diesel engines to decrease the amount of nitrogen oxides in exhaust gas. *J. Mar. Sci. Technol.* **2015**, *20*, 393–405. [[CrossRef](#)]
38. Uyumaz, A. An experimental investigation into combustion and performance characteristics of an HCCI gasoline engine fueled with n-heptane, isopropanol and n-butanol fuel blends at different inlet air temperatures. *Energy Convers. Manag.* **2015**, *98*, 199–207. [[CrossRef](#)]
39. Calam, A.; Aydoğan, B.; Halis, S. The comparison of combustion, engine performance and emission characteristics of ethanol, methanol, fusel oil, butanol, isopropanol and naphtha with n-heptane blends on HCCI engine. *Fuel* **2020**, *266*, 117071. [[CrossRef](#)]
40. Sivasubramanian, H.; Pochareddy, Y.K.; Dhamodaran, G.; Esakkimuthu, G.S. Performance, emission and combustion characteristics of a branched higher mass, C 3 alcohol (isopropanol) blends fuelled medium duty MPFI SI engine. *Eng. Sci. Technol. Int. J.* **2017**, *20*, 528–535. [[CrossRef](#)]
41. Baloch, H.A.; Nizamuddin, S.; Siddiqui, M.; Riaz, S.; Jatoi, A.S.; Dumbre, D.K.; Mubarak, N.; Srinivasan, M.; Griffin, G. Recent advances in production and upgrading of bio-oil from biomass: A critical overview. *J. Environ. Chem. Eng.* **2018**, *6*, 5101–5118. [[CrossRef](#)]
42. Dominković, D.F.; Bačeković, I.; Pedersen, A.S.; Krajačić, G. The future of transportation in sustainable energy systems: Opportunities and barriers in a clean energy transition. *Renew. Sustain. Energy Rev.* **2018**, *82*, 1823–1838. [[CrossRef](#)]
43. Trumbo, J.L.; Tonn, B.E. Biofuels: A sustainable choice for the United States' energy future? *Technol. Forecast. Soc. Chang.* **2016**, *104*, 147–161. [[CrossRef](#)]
44. Abbas, S.Z.; Kousar, A.; Razzaq, S.; Saeed, A.; Alam, M.; Mahmood, A. Energy management in South Asia. *Energy Strat. Rev.* **2018**, *21*, 25–34. [[CrossRef](#)]
45. Patel, P.D.; Lakdawala, A.; Chourasia, S.K.; Patel, R. Bio fuels for compression ignition engine: A review on engine performance, emission and life cycle analysis. *Renew. Sustain. Energy Rev.* **2016**, *65*, 24–43. [[CrossRef](#)]
46. Thangavelu, S.K.; Ahmed, A.S.; Ani, F.N. Review on bioethanol as alternative fuel for spark ignition engines. *Renew. Sustain. Energy Rev.* **2016**, *56*, 820–835. [[CrossRef](#)]
47. Imran, S.; Emberson, D.; Wen, D.; Diez, A.; Crookes, R.; Korakianitis, T. Performance and specific emissions contours of a diesel and RME fueled compression-ignition engine throughout its operating speed and power range. *Appl. Energy* **2013**, *111*, 771–777. [[CrossRef](#)]
48. Luo, H.; Zheng, P.; Bilal, M.; Xie, F.; Zeng, Q.; Zhu, C.; Yang, R.; Wang, Z. Efficient bio-butanol production from lignocellulosic waste by elucidating the mechanisms of *Clostridium acetobutylicum* response to phenolic inhibitors. *Sci. Total. Environ.* **2020**, *710*, 136399. [[CrossRef](#)] [[PubMed](#)]
49. Çelebi, Y.; Aydın, H. An overview on the light alcohol fuels in diesel engines. *Fuel* **2019**, *236*, 890–911. [[CrossRef](#)]
50. Yilmaz, N.; İleri, E.; Atmanlı, A. Performance of biodiesel/higher alcohols blends in a diesel engine. *Int. J. Energy Res.* **2016**, *40*, 1134–1143. [[CrossRef](#)]
51. Markov, V.A.; Gaivoronsky, A.I.; Grechov, L.V.; Ivashchenko, N.A. *Work of diesel engines on alternative fuels (Работа дизелей на нетрадиционных топливах)*-In Russian; Legion-Avtodata: Moscow, Russia, 2008; ISBN 978-5-88850-361-4.
52. Rimkus, A.; Žaglinskis, J.; Stravinskas, S.; Rapalis, P.; Matijošius, J.; Bereczky, A. Research on the Combustion, Energy and Emission Parameters of Various Concentration Blends of Hydrotreated Vegetable Oil Biofuel and Diesel Fuel in a Compression-Ignition Engine. *Energies* **2019**, *12*, 2978. [[CrossRef](#)]
53. Rimkus, A.; Pukalskas, S.; Matijošius, J.; Sokolovskij, E. Betterment of ecological parameters of a diesel engine using Brown's gas. *J. Environ. Eng. Landsc. Manag.* **2012**, *21*, 133–140. [[CrossRef](#)]
54. Fuć, P.; Lijewski, P.; Ziolkowski, A.; Dobrzyński, M. Dynamic Test Bed Analysis of Gas Energy Balance for a Diesel Exhaust System Fit with a Thermoelectric Generator. *J. Electron. Mater.* **2017**, *46*, 3145–3155. [[CrossRef](#)]
55. JCGM 100 2008. Evaluation of measurement data—Guide to the expression of uncertainty in measurement. Available online: [https://www.bipm.org/utis/common/documents/jcgm/JCGM\\_100\\_2008\\_E.pdf](https://www.bipm.org/utis/common/documents/jcgm/JCGM_100_2008_E.pdf) (accessed on 13 April 2020).

56. Evaluation of measurement data—Supplement 1 to the “Guide to the expression of uncertainty in measurement”—Propagation of distributions using a Monte Carlo method. Available online: [https://www.bipm.org/utis/common/documents/jcgm/JCGM\\_101\\_2008\\_E.pdf](https://www.bipm.org/utis/common/documents/jcgm/JCGM_101_2008_E.pdf) (accessed on 27 April 2020).
57. Gutarevych, Y.; Mateichyk, V.; Matijošius, J.; Rimkus, A.; Gritsuk, I.; Syrota, O.; Shuba, Y. Improving Fuel Economy of Spark Ignition Engines Applying the Combined Method of Power Regulation. *Energies* **2020**, *13*, 1076. [[CrossRef](#)]
58. Zöldy, M. Fuel Properties of Butanol–Hydrogenated Vegetable Oil Blends as a Diesel Extender Option for Internal Combustion Engines. *Period. Polytech. Chem. Eng.* **2019**, *64*, 205–212. [[CrossRef](#)]
59. Zöldy, M. Investigation of Correlation Between Diesel Fuel Cold Operability and Standardized Cold Flow Properties. *Period. Polytech. Transp. Eng.* **2019**. [[CrossRef](#)]
60. Kumar, S.; Pandey, A.K. Current Developments in Biotechnology and Bioengineering and Waste Treatment Processes for Energy Generation. *Curr. Dev. Biotechnol. Bioeng.* **2019**, 1–9. [[CrossRef](#)]
61. Zöldy, M. Improving Heavy Duty Vehicles Fuel Consumption with Density and Friction Modifier. *Int. J. Automot. Technol.* **2019**, *20*, 971–978. [[CrossRef](#)]
62. Ghosh, P.; Jaffe, S.B. Detailed Composition-Based Model for Predicting the Cetane Number of Diesel Fuels. *Ind. Eng. Chem. Res.* **2006**, *45*, 346–351. [[CrossRef](#)]
63. Gutarevych, Y.; Shuba, Y.; Matijošius, J.; Karev, S.; Sokolovskij, E.; Rimkus, A. Intensification of the combustion process in a gasoline engine by adding a hydrogen-containing gas. *Int. J. Hydrog. Energy* **2018**, *43*, 16334–16343. [[CrossRef](#)]
64. Kukharonak, H.; Ivashko, V.; Pukalskas, S.; Rimkus, A.; Matijošius, J. Operation of a Spark-ignition Engine on Mixtures of Petrol and N-butanol. *Procedia Eng.* **2017**, *187*, 588–598. [[CrossRef](#)]
65. Zöldy, M.; Hollo, A.; Thernes, A. Butanol as a Diesel Extender Option for Internal Combustion Engines. *SAE Tech. Paper Ser.* **2010**. [[CrossRef](#)]
66. Hunicz, J.; Matijošius, J.; Rimkus, A.; Kilikevičius, A.; Kordos, P.; Mikulski, M. Efficient hydrotreated vegetable oil combustion under partially premixed conditions with heavy exhaust gas recirculation. *Fuel* **2020**, *268*, 117350. [[CrossRef](#)]
67. Caban, J.; Drożdździał, P.; Ignaciuk, P.; Kordos, P. THE IMPACT OF CHANGING THE FUEL DOSE ON CHOSEN PARAMETERS OF THE DIESEL ENGINE START-UP PROCESS. *Transp. Probl.* **2019**, *14*, 51–62. [[CrossRef](#)]
68. Kilikevičienė, K.; Kačianauskas, R.; Kilikevičius, A.; Maknickas, A.; Matijošius, J.; Rimkus, A.; Vainorius, D. Experimental investigation of acoustic agglomeration of diesel engine exhaust particles using new created acoustic chamber. *Powder Technol.* **2020**, *360*, 421–429. [[CrossRef](#)]
69. Rimkus, A.; Matijošius, J.; Bogdevicius, M.; Bereczky, A.; Török, Á. An investigation of the efficiency of using O<sub>2</sub> and H<sub>2</sub> (hydroxile gas -HHO) gas additives in a ci engine operating on diesel fuel and biodiesel. *Energy* **2018**, *152*, 640–651. [[CrossRef](#)]
70. Zavadskas, E.K.; Čereška, A.; Matijošius, J.; Rimkus, A.; Baušys, R. Internal Combustion Engine Analysis of Energy Ecological Parameters by Neutrosophic MULTIMOORA and SWARA Methods. *Energies* **2019**, *12*, 1415. [[CrossRef](#)]
71. Zöldy, M. Potential future renewable fuel challenges for internal combustion engine. *Járművek és Mobilgépek II. évf* **2009**, *2*, 397–403.
72. Lijewski, P.; Fuć, P.; Dobrzynski, M.; Markiewicz, F. Exhaust emissions from small engines in handheld devices. *MATEC Web Conf.* **2017**, *118*, 16. [[CrossRef](#)]

